HHS Public Access

Author manuscript

Lab Invest. Author manuscript; available in PMC 2023 September 19.

Published in final edited form as:

Lab Invest. 2023 February ; 103(2): 100018. doi:10.1016/j.labinv.2022.100018.

Loss of Protein Kinase D2 Activity Protects Against Bleomycin-Induced Dermal Fibrosis in Mice

Liping Chen[a], **Jinjun Zhao**[b], **Yapeng Chao**[c], **Adhiraj Roy**[d], **Wenjing Guo**[a], **Jiabi Qian**[a], **Wanfu Xu**[a], **Robyn T. Domsic**[e], **Robert Lafyatis**[e], **Binfeng Lu**[f], **Fan Deng**[a,*], **Q. Jane Wang**[c,*]

[a]Department of Cell Biology, School of Basic Medical Sciences, Southern Medical University, Guangzhou, China

[b]Department of Rheumatology, Nanfang Hospital, Southern Medical University, Guangzhou, China

[c]Department of Pharmacology and Chemical Biology, University of Pittsburgh, Pittsburgh, Pennsylvania

[d]Amity Institute of Molecular Medicine and Stem Cell Research, Amity University, Noida, India

[e]Department of Medicine, Division of Rheumatology and Clinical Immunology, University of Pittsburgh, Pittsburgh, Pennsylvania

[f]Department of Immunology, University of Pittsburgh, Pittsburgh, Pennsylvania

Abstract

Protein kinase D (PKD) has been linked to inflammatory responses in various pathologic conditions; however, its role in inflammation-induced dermal fibrosis has not been evaluated. In this study, we aimed to investigate the roles and mechanisms of protein kinase D2 (PKD2) in inflammation-induced dermal fibrosis and evaluate the therapeutic potential of PKD inhibitors in this disease. Using homozygous kinase-dead PKD2 knock-in (KI) mice, we examined whether genetic ablation or pharmacologic inhibition of PKD2 activity affected dermal inflammation and fibrosis in a bleomycin (BLM)-induced skin fibrosis model. Our data showed that dermal thickness and collagen fibers were significantly reduced in BLM-treated PKD2 KI mice compared with that in wild-type mice, and so was the expression of α-smooth muscle actin and collagens and the mRNA levels of transforming growth factor-β1 and interleukin-6 in the KI mice.

*Corresponding author. fandeng@smu.edu.cn (F. Deng), qjw1@pitt.edu (Q.J. Wang).

These authors contributed equally: Liping Chen and Jinjun Zhao.

Author Contributions

Q.J.W. and F.D. conceptualized the study. L.C., J.Z., Y.C., A.R., and B.L. conceived the methodology of the study. L.C., J.Z., Y.C., A.R., W.G., J.Q., W.X., B.L., and Q.J.W. performed the data and experimental analysis. Q.J.W., B.L., R.L., and F.D. procured the resources. L.C. and J.Z. wrote and prepared the original draft. L.C., J.Z., A.R., R.T.D, and R.L., Q.J.W., B.L., and F.D. reviewed and edited the manuscript. Q.J.W. and F.D. supervised the study. Q.J.W. managed the funding acquisition. All authors have read and agreed to the published version of the manuscript

Declaration of Competing Interest

The authors state no conflict of interest.

Ethics Approval and Consent to Participate

All animal protocols were approved by the Institutional Animal Care and Use Committees at the University of Pittsburgh and the Southern Medical University, and the experiments were performed following relevant guidelines.

Supplementary Material

The online version contains supplementary material available at https://doi.org/10.1016/j.labinv.2022.100018.

Corroboratively, pharmacologic inhibition of PKD by CRT0066101 also significantly blocked BLM-induced dermal fibrosis and reduced α-smooth muscle actin, collagen, and interleukin-6 expression. Further analyses indicated that loss of PKD2 activity significantly blocked BLM-induced infiltration of monocytes/macrophages and neutrophils in the dermis. Moreover, using bone marrow–derived macrophages, we demonstrated that PKD activity was required for cytokine production and migration of macrophages. We have further identified Akt as a major downstream target of PKD2 in the early inflammatory phase of the fibrotic process. Taken together, our findings indicate that PKD2 promotes dermal fibrosis via regulating immune cell infiltration, cytokine production, and downstream activation of Akt in lesional skin, and targeted inhibition of PKD2 may benefit the treatment of this condition.

Keywords

dermal fibrosis; protein kinase D; bleomycin; macrophage; systemic sclerosis; Akt

Introduction

Dermal fibrosis is associated with several diseases, most notably systemic sclerosis (SSc), which is a complex multisystem connective tissue disease with high mortality.[1] Following the early inflammatory stage of SSc, tissue deposition of collagen-rich scar occurs, disrupting the normal architecture of the skin and leading to the dysfunction and eventual failure of the skin, lung, and other organs.[2] The treatments for SSc are often symptomatic and have limited effectiveness. Novel targets and treatments are urgently needed.

Inflammation and fibrosis are intimately coupled during the progression of tissue fibrosis. Advances in the past few years have led to the identification of many important inflammatory and fibrotic mediators, such as transforming growth factor-β1 (TGF-β1) and interleukin-6 (IL-6), which play key roles in the pathogenesis of dermal fibrosis. Several experimental dermal fibrosis models have been developed that bore resemblance to that occurring in human SSc.[3] Among them, the bleomycin (BLM)-induced fibrosis model is most widely used. It is well established that mice receiving daily subcutaneous (s.c.) injections of BLM for 4 to 6 weeks develop dermal fibrosis with autoantibody production and immune infiltration, which mimic the biochemical and histologic features of human SSc.[4,5] Thus, we have chosen this model to examine the role of protein kinase D (PKD) in dermal fibrosis associated with SSc.

PKD belongs to a subfmaily of the Ca^{2+}/calmodulin-dependent protein kinase superfamily, with 3 different isoforms having been identified: PKD1, PKD2, and PKD3,[6,7] with PKD1 being the most extensively studied isoform. PKD plays an important role in a variety of cellular processes, including cell proliferation, migration, secretion, and inflammation.[7,8] Its involvement in the inflammatory process has been implicated in several studies. PKD is required for the production of proinflammatory cytokines and chemokines in tumor cells,[9] immune cells,[10–12] and endothelial cells in response to various stimuli.[13] PKD has been implicated in the following inflammatory conditions: pancreatitis, hypersensitivity pneumonitis,[10] autoimmune diseases, allergic inflammatory diseases, viral infections,

airway inflammation, and Sjögren syndrome–related inflammation.[8,10,12,14–20] PKD has also been implicated in heart and lung fibrosis[21,22] and idiopathic pulmonary fibrosis[22]; however, its role in dermal fibrosis has not been examined.

In this study, we found that knock-in (KI) of kinase-dead PKD2 or inhibition of PKD activity prevented dermal fibrosis in a BLM-induced fibrosis mouse model. We showed that KI mice or PKD inhibitor–treated mice exhibited reduced dermal thickness and decreased α-smooth muscle actin (α-SMA) expression, collagen deposition, and production of proinflammatory/profibrotic mediators in response to BLM treatment *in vivo*. We further identified PKD-expressing cells in the dermis of BLM-treated mouse skin. Our study demonstrated the potentially critical role of this kinase family in BLM-induced dermal fibrosis through modulating immune infiltration and cytokine production.

Materials and Methods

Reagents

The following antibodies were obtained from Cell Signaling Technology: PKD1, PKD2, PKD3 (D57E6 Rabbit mAb), p-PKD1 (Ser916), CD45, CD68, and α-Smooth Muscle Actin. p-PKD2 (Ser876) and eBioscience 1X RBC Lysis Buffer were obtained from Thermo Fisher. TrueBlack Lipofuscin Autofluorescence Quencher was obtained from Biotium. Donkey anti-Rabbit IgG (H+L) Highly Cross-Adsorbed Secondary Antibody, Alexa Fluor 488, Donkey anti-Rabbit IgG (H+L) Highly Cross-Adsorbed Secondary Antibody, Alexa Fluor 568, and Mouse M-CSF Recombinant Protein were obtained from Invitrogen. Lipopolysaccharides (LPS) from *Escherichia coli* O111:B4 were purchased from Sigma. Bleomycin hydrochloride was purchased from Nippon Kayaku.

PKD2$^{SSAA/SSAA}$-Knock-in Mice

Catalytic deficient heterozygous PKD2$^{S707A/S711A/WT}$-KI (PKD2$^{SSAA/WT}$-KI) mice on a C57BL/6 background were obtained from Jackson Laboratory. Six-week-old male PKD2 wild-type (WT) mice and PKD2$^{SSAA/WT}$-KI mice (body weight, approximately 20 g) were maintained with food and water ad libitum and housed in specific pathogen-free conditions. Mouse genotyping was performed by the PCR amplification of genomic DNA.[23] Homozygous PKD2$^{SSAA/SSAA}$-KI mice were obtained by intercrossing heterozygous PKD2$^{SSAA/WT}$ mice.[24] Mice used in the study were housed in specific pathogen-free conditions. All animal protocols were approved by the Institutional Animal Care and Use Committees at the University of Pittsburgh and the Southern Medical University, and the experiments were performed following relevant guidelines.

Bleomycin-Induced Dermal Fibrosis Model and Mouse Tissue Sample Preparation

To induce dermal fibrosis, 6- to 8-week-old healthy WT and PKD2$^{SSAA/SSAA}$ (PKD2-KI) mice (matched in sex, age, and weight) were subjected to subcutaneous (s.c.) injection of BLM (100 μL at 1 mg/mL) daily at a shaved area (~3 cm^2) on the back for 4 weeks as described,[5,25] and the control mice received 100 μL of phosphate-buffered saline (PBS). To measure lymphocyte infiltration, WT and PKD2-KI mice were injected s.c. with BLM (100 μL at 1 mg/mL) for 1 week. The skin tissues at the lesion site were collected for

immunohistochemical (IHC) analysis. For the PKD inhibitor treatment, healthy female WT C57BL/6 mice (6–8 weeks old) were administered CRT0066101 (CRT) orally at 80 mg/kg in a 5% dextrose saline solution every day for 4 weeks. Mouse weight was measured once weekly. Mouse group allocation was blinded at all stages of experiments and analyses. Based on the literature and our preliminary data, a sample size of 6 to 9 mice per group was needed to have 80% power to detect the difference in mean values (effect size = 2.4) between experimental and control groups, with a significance level of 0.05. All mice and data points in each experimental group were included in the analysis.

To collect tissues, mice were anesthetized and hair was removed at BLM injection sites, and the dorsal skin was carefully dissected by RNA-free surgical scissors and divided into 3 parts: 1 was fixed in neutral buffered formalin (10%) for paraffin embedding, sectioning, hematoxylin and eosin (H&E) staining, and immunohistochemical analysis; 1 was embedded in optimal cutting temperature compound and flash frozen for sectioning and immunofluorescence (IF) staining; and the remaining, after eliminating the subcutaneous fat layer, was snap frozen in liquid N_2 and stored at −80 °C for Western blotting and real-time reverse-transcription PCR (RT-qPCR) analysis.

Western Blotting Analysis and IF Staining

Please refer to Supplementary Methods for details.

RNA Extraction and RT-qPCR Analysis

Total RNA was extracted from tissues using TRIzol reagent (Invitrogen) following the manufacturer's protocol. RNA extraction and RT-qPCR analysis were performed as described.[26] Please refer to Supplementary Methods for a detailed description and the list of qPCR primers used (Supplementary Table S1).

Bone Marrow–Derived Macrophage Preparation

The femur and tibia of WT C57BL/6 mice were dissected. Bone marrow was flushed with 10 mL of RPMI-1640 medium and centrifuged at 1200 rpm for 5 minutes. The supernatant was discarded and cell pellets were treated with eBioscience1× RBC Lysis Buffer. After washing, the cells were cultured in RPMI-1640 medium supplemented with 10 % fetal bovine serum and mouse macrophage colony-stimulating factor (Thermo Fisher). The medium was replenished every 3 days and day-6 macrophages were used for the experiment.

Statistical Analysis

The power and sample size analyses were conducted using G*Power software.[27] Statistical analysis was performed using SPSS 21.0 software (SPSS) using the independent sample *t* test or analysis of variance with pairwise comparisons using the Dunnett, Fisher, or Tukey test. Median values were evaluated using the Kruskal-Wallis test, and pairwise comparisons were performed using the Mann-Whitney test. Replicate experiments were analyzed both independently and jointly, controlling for batch effects. Data are presented as the mean ± SEM. A *P* value <.05 was considered as significant.

Results

Knock-in of Kinase-Dead PKD2 Blocked Bleomycin-Induced Mouse Dermal Fibrosis

Homozygous PKD2$^{SSAA/SSAA}$-KI mice were generated by replacing WT PKD2 alleles with mutant alleles that encode alanine substitutions of Ser707 and Ser711 (S707A/S711A) in the activation loop of PKD2 (Supplementary Fig. S1A). The phosphorylation of the 2 conserved serine residues in the activation loop is essential for PKD activity.[28] This mouse model was first reported by Matthews et al.[23] The homozygous mice were viable, fertile, normal in size, and did not display any gross physical or behavioral abnormalities. Mouse genotyping confirmed the presence of mutated alleles in the KI mice (Supplementary Fig. S1B), and Western blotting demonstrated an absence of PKD2 activity measured by p-PKD2 (ser876) antibody in various tissues (Supplementary Fig. S1C).

An s.c. injection of 100 μL BLM at 1 mg/mL daily for 28 days leads to dermal fibrosis in mice, which is characterized by infiltration of mononuclear cells into the lesional skin and thickening of the dermis that is maintained for at least 6 weeks after cessation of the treatment.[4,25] To investigate the role of PKD2 in this process, mice were randomized into 4 groups that received either vehicle (1x PBS at 100 μL/mouse, once daily) or BLM (100 μL at 1 mg/mL, once daily) (n = 9 mice, total 36 mice): PKD2$^{WT/WT}$-PBS, PKD2$^{WT/WT}$-BLM, PKD2$^{SSAA/SSAA}$-PBS, and PKD2$^{SSAA/SSAA}$-BLM (Fig. 1A). Dermal thickness is a crucial indicator of dermal fibrosis.[29] Histopathological analysis of H&E-stained skin sections from the 4 groups of mice showed that dermal thickness was increased by more than 2-fold in response to BLM in PKD2$^{WT/WT}$ mice compared with that in vehicle-treated mice, whereas this response was significantly reduced in the PKD2$^{SSAA/SSAA}$-KI mice receiving BLM injection (Fig. 1B, C). Additionally, the effect was observed only in the dermal layer, but not in the epidermal layer, which agrees with other reports[30] (Fig. 1C, D). Altogether, we showed that the inactivation of PKD2 as in PKD2$^{SSAA/SSAA}$-KI mice blocked dermal thickening in a BLM-induced dermal fibrosis mouse model.

Inactivation of PKD2 Significantly Abated Collagen Fiber Expression in Bleomycin-Treated Mouse Dermis

Fibrosis is characterized by an excessive deposition of extracellular matrix (ECM) components such as collagens and fibronectin.[31,32] We examined collagen fibers using Masson trichrome staining. As shown in Figure 2, the dermal layers in the PKD2$^{SSAA/SSAA}$-BLM group were arranged normally; however, the collagen fiber staining was weaker in the PKD2$^{SSAA/SSAA}$ mice compared with that in the PKD2$^{WT/WT}$ mice treated with BLM (Fig. 2A). Quantitative analysis indicated that the BLM-induced collagen fiber deposition was greatly reduced in the PKD2$^{SSAA/SSAA}$-BLM group compared with that in the control PKD2$^{WT/WT}$-BLM group (Fig. 2B). Thus, PKD2 catalytic activity was required for BLM-induced collagen deposition in the dermis.

The Levels of α-SMA, Collagen, and Profibrotic/Proinflammatory Cytokines Were Significantly Reduced in the Dermis of Bleomycin-Treated Knock-in Mice

Myofibroblasts, a key player in the fibrotic process, are differentiated forms of fibroblasts that have features of both smooth muscle cells and fibroblasts. They are characterized by the

expression of α-SMA.[33] In this study, we examined the expression of α-SMA and collagens in PKD2$^{WT/WT}$ and PKD2$^{SSAA/SSAA}$ mice. As shown in Figure 2C, mRNA levels of α-SMA were decreased in PKD2$^{SSAA/SSAA}$ mice treated with or without BLM compared with those in PKD2$^{WT/WT}$ mice. Additionally, the mRNA expressions of collagen I, collagen IV-α1, and collagen IV-α2 were reduced in BLM- and vehicle-treated PKD2$^{SSAA/SSAA}$ mice compared with those in PKD2$^{WT/WT}$ mice (Fig. 2C). Importantly, the levels of 2 main proinflammatory and profibrotic cytokines, IL-6 and TGF-β1, induced by BLM in PKD2$^{WT/WT}$ mice, were also significantly reduced in PKD2$^{SSAA/SSAA}$ mice treated with or without BLM (Fig. 2D). It should be noted that although the loss of PKD2 activity did not abolish BLM-induced *α*-SMA, collagen, TGF-β1, and IL-6 expression, the fold inductions of these genes following BLM treatment in PKD2$^{SSAA/SSAA}$ mice were lower than those in PKD2$^{WT/WT}$ mice, especially in terms of TGF-β1 and IL-6 (Fig. 2D). Thus, PKD2 activity is required for the induction of proinflammatory and profibrotic cytokines in BLM-induced dermal fibrosis.

Further analyses indicated that BLM failed to induce α-SMA protein expression in PKD2$^{SSAA/SSAA}$-BLM mice ($P < .01$) (Fig. 3A, B). Similarly, the protein level of collagen I-α2 was also decreased in PKD2$^{SSAA/SSAA}$ mice treated with BLM compared with the control group (Fig. 3A, B). In contrast, the levels of PKD1, PKD2, and PKD3 proteins and transcripts remained constant in all 4 groups of mice (Fig. 3A, C), whereas no p-PKD2 (S876) was detected in the dermis and epidermis of PKD2$^{SSAA/SSAA}$ mice compared with that in PKD2$^{WT/WT}$ mice (Fig. 3A). Mouse skin sections were further analyzed for the presence of myofibroblasts, a key player in the fibrotic process after BLM treatment. As shown in Figure 3D, there were a significantly reduced number of α-SMA–positive cells in the dermis of KI mice compared with that in WT mice after 4 weeks of BLM treatment, which is in line with the Western blotting results (Fig. 3A). Taken together, our data indicate that PKD2 activity is necessary for α-SMA and collagen I-α2 expression in the dermis of BLM-treated mice.

Inhibition of PKD Blocked Bleomycin-Induced Dermal Fibrosis in Mice

To further corroborate our findings in mouse genetic models and exploit the therapeutic potential of targeting PKD, we investigated whether targeted inhibition of PKD using small-molecule inhibitors has an impact on BLM-induced dermal fibrosis. CRT is an orally available potent PKD inhibitor with demonstrated *in vivo* activity in multiple animal models.[34–36] Female mice (7 weeks old) were randomized into 3 groups (n = 6, total 18 mice) to receive daily s.c. injections of vehicle (1x PBS,100 μL/mouse), BLM (100 μL at 1 mg/mL), and BLM + CRT (80 mg/kg, orally, once daily). H&E-stained skin sections from the 3 groups of mice showed that while dermal thickness was significantly increased (approximately 1.5-fold) in response to BLM treatment compared with vehicle-treated mice, CRT completely blocked this effect of BLM in the dermis (Fig. 4A, B). Additionally, as described above, the effect was observed only in the dermal layer but not in the epidermal layer (Fig. 4B).

The expression of α-SMA and collagens (collagen I, collagen IV-α1, and collagen IV-α2) was examined in the skin samples collected from the 3 groups of mice. As shown in

Figure 4C, the mRNA levels of these genes were increased in response to BLM treatment, although significantly reduced by CRT, compared with those in the vehicle-treated control group. Similarly, BLM-induced IL-6 was also significantly blocked by CRT (Fig. 4C). Taken together, the inhibition of PKD by CRT reduced BLM-induced dermal fibrosis in mice.

Distinct Patterns of PKD Expression in Mouse Skin and the Role of PKD2 in Monocyte/Macrophage Infiltration in the Lesional Skin

To provide insights into how PKDs regulate skin function, we examined the distribution of the 3 PKD isoforms in the skin of BLM-treated mice using IF staining. As shown in Figure 5A, skin sections from mice treated with or without BLM showed distinct patterns of PKD1/2/3 distribution. PKD1 showed widespread distribution in both the epidermis and dermis, with predominant expression in the epidermis. After BLM treatment, the expression of PKD1 increased in the dermis. Interestingly, the adipose tissue layer in the hypodermis also showed prominent expression of PKD1 after BLM treatment. In contrast, PKD2 expression was found in discrete regions or sporadic cells/cell clusters within the dermis. In BLM-treated skin, there was an increased number of PKD2-positive sporadic cells in the dermis. In comparison, PKD3 was mainly detected in hair follicle-like structures within the dermis before and after BLM treatment. Thus, PKD isoforms reside in distinct regions/cell types in the skin, suggesting that they may play different roles in BLM-induced dermal fibrosis.

To gain further understanding of the function of PKD2 in BLM-induced fibrosis, we sought to determine the identity of PKD2-positive cells in the skin of BLM-treated mice. CD45 and CD68, which are markers of the myeloid lineage, were costained with PKD2 in skin sections from BLM-treated mice at 4 weeks. As shown in Figure 5B, PKD2-positive signals nearly overlapped with those of CD45 and CD68. These data indicated that PKD2-positive cells likely belonged to the myeloid lineage. To determine whether PKD2 activity affects immune cell infiltration, a critical event at the onset of inflammation leading to fibrosis, KI and WT mice were subjected to daily s.c. injection of BLM (1 mg/mL) for 7 days, and skin tissues were collected and subjected to IF staining for infiltrated immune cells, including monocytes/macrophages (F4/80, CD68, and CD11b) and neutrophils (Ly68), all key players in the inflammatory process. Our data demonstrated that the number of infiltrated F4/80+ (Fig. 5C, D), CD68+ (Supplementary Fig. S2A), and CD11b+ (Supplementary Fig. S2B) monocytes/macrophages and Ly68+ (Supplementary Fig. S2C, D) neutrophils in the dermis of BLM-treated KI mice were significantly reduced compared with that in WT mice, indicating that PKD2 activity is required for the recruitment of proinflammatory immune cells at the skin lesional site.

Loss of PKD2 Activity Was Required for the Migration and Cytokine Production of Bone Marrow–Derived Macrophages

Our data implied that PKD2 was predominantly expressed in cells of the myeloid lineage that can reside or be recruited to the lesional skin of BLM-treated mice. A major population of the myeloid cells marked by CD45/CD68 is macrophages, which have been implicated in the pathogenesis of dermal fibrosis in SSc. To determine if PKD affects the function of macrophages, we obtained bone marrow–derived macrophages (BMMs) from WT mice.

The role of PKD in BMM migration and cytokine production, the 2 critical functions of macrophages that contribute to the pathogenesis of dermal inflammation and fibrosis, was examined. As shown in Figure 6A, BMM expressed all the 3 PKD isoforms, with PKD1 being the most predominant. By costaining for PKD1 and CD68, we confirmed that the BMM we obtained expressed the macrophage marker CD68, and PKD1 was well colocalized with CD68 (Fig. 6B), as observed in tissue sections. Next, BMM was stimulated with LPS, a potent activator of macrophages and a systemic inflammatory stimulator, to induce cytokine production. LPS induced the activation of PKD1, which can be detected at 2 hours and peaked at 4 hours, and returned to the baseline at 12 hours (Fig. 6C). PKD2 was activated with similar kinetics (data not shown). The effect of PKD inhibition or depletion on the production of cytokine TGF-β1 was examined following LPS stimulation. The inhibition of PKD by CRT potently blocked the induction of TGF-β1 by LPS (Fig. 6D). Accordingly, the knockdown of PKD1 or PKD2 also partially blocked LPS-induced TGF-β1 production (Fig. 6E). Finally, the effect of PKD inhibition on BMM migration was examined in the presence or absence of CRT. As shown in Figure 6F, CRT decreased the migratory activity of BMM by 2-fold. Taken together, PKD activity is required for the migration and production of cytokines in macrophages. Our findings imply that PKD may contribute to BLM-induced fibrosis by promoting the recruitment and production of cytokines from macrophages.

Genetic Inactivation of PKD2 Blocked BLM-Induced Akt Activation in the Early Inflammatory Phase of Dermal Fibrosis

To gain insights into the signaling events downstream of PKD2, we examined the expression and activity of Akt and Stat3, both known to be activated in response to TGF-β1 and IL-6, which were downregulated in the PKD2-KI mice (Figs. 2 and 4). In particular, IL-6 signals through the canonical JAK/Stat3 signaling pathway to regulate the inflammatory process. As shown in Figure 7, BLM caused the upregulation and activation (measured by p-S473-Akt and p-Y705-Stat3) of Akt and Stat3 in the WT mouse skins collected 1 week after BLM treatment. However, in the corresponding KI mouse skins, despite the increased basal expression of Akt and Stat3, BLM failed to induce Akt activation, as indicated by the low p-S473-Akt level in BLM-treated KI skins (Fig. 7A, B). In contrast, the level of p-Y705-Stat3 remained constant in BLM- vs vehicle-treated KI mouse skins, implying that the loss of PKD2 activity blocked BLM-induced Akt activation but did not affect that of Stat3, despite their upregulation at the basal level. Taken together, these findings indicate that PKD2 activity is required for BLM-induced Akt activation during the early inflammatory phase of dermal fibrosis.

Discussion

Dermal fibrosis can occur in a variety of human diseases, most notably SSc, which is a complex multisystem autoimmune disease that has the highest case-specific mortality of connective tissue illnesses.[37] Although significant advances have been made in the diagnosis and treatment of SSc, the molecular basis of the disease remains largely elusive and no Food and Drug Administration–approved therapies are available.[38,39] Although PKD has been implicated in fibrosis and inflammation,[8,21,22,40] its role in dermal fibrosis involved

in SSc has not been investigated. In this study, using a KI mouse model of kinase-dead PKD2, we demonstrated that genetic ablation of PKD2 activity protected mice from BLM-induced dermal fibrosis, indicating the critical role of PKD2 activity in this pathologic condition. Figure 8 depicts the potential mechanism through which PKD2 contributes to dermal fibrosis.

Dermal fibrosis is characterized by the hardening and thickening of the dermal layer in the skin, in part caused by the excessive accumulation of ECM, which contributes to fibrosis development. Activated fibroblasts (myofibroblasts) are known to be the main type of cells responsible for the overproduction of collagens and other ECM components.[41] The interactions between fibroblasts and inflammatory cells and the production of proinflammatory cytokines by the inflammatory cells play a crucial role in the induction of myofibroblastic activity.[42] TGF-β1, a key regulator of fibrosis, has been shown to[43] mediate fibroblast proliferation,[44] collagen production,[45] ECM deposition, and myofibroblast differentiation in dermal fibrosis. The enhanced expression of TGF-β1 stimulates collagen synthesis in fibroblasts by activating the smad2/3 signaling pathway,[46] resulting in the overabundant accumulation of collagen.[47] Additionally, at the early stages of SSc, a high level of IL-6 was associated with diffuse cutaneous SSc, increased levels of inflammatory markers, more severe skin fibrosis, and worse long-term survival.[48]

To determine whether there is a relationship between dermal fibrosis and PKD2, we obtained homozygous PKD2$^{SSAA/SSAA}$-KI mice in which PKD2 activity was eliminated by mutating S707/S711 in the activation loop of PKD2. Our results showed that loss of PKD2 activity significantly blocked the BLM-induced dermal thickening and reduced collagen and a-SMA protein expression in the dermis of BLM-treated KI mice. Interestingly, PKD2-KI mice also showed significantly reduced collagen and α-SMA expression under the basal state without BLM treatment, as compared with the WT mice, suggesting the fundamental role of PKD2 in regulating α-SMA expression. In WT mice, repeated BLM injections caused the infiltration of inflammatory cells and increased myofibroblastic activity, fibrosis, and thickening of the skin. In contrast, PKD2-KI mice showed reduced deposition of collagen in the skin, decreased dermal thickening, and reduced fibrosis. TGF-β1 and IL-6 mRNA levels were also decreased in BLM-treated KI mice relative to WT mice. These results confirm the essential role of the proinflammatory and profibrotic properties of PKD2 in BLM-induced dermal fibrosis in mice, implying that PKD may be a potential therapeutic target for skin fibrosis and SSc. Further analyses indicate that PKD2-positive cells were largely myeloid cells that could be recruited to the lesional skin to promote the fibrotic process via the production of profibrotic cytokines, including TGF-β1. Thus, PKD2 activity is required for both the recruitment of monocytes/macrophages and the production of proinflammatory and profibrotic cytokines from these immune cells at the lesional sites, implying the dual role of PKD2 in dermal fibrosis. Further analyses have identified Akt as a major downstream target of PKD2 in the early inflammatory phase of the fibrotic process. The genetic inactivation of PKD2 blocked BLM-induced Akt activation, but not that of Stat3, in mouse dermis. Akt is a critical signaling node of fibrogenesis in many organs, including SSc.[49,50] Profibrotic cytokines and growth factors, such as TGF-β1, IL-6, and epidermal growth factor, can activate the PI3K/Akt signaling pathway in myofibroblasts to promote tissue remodeling and scarring.[51,52] Notably, it has been demonstrated that

Akt is activated in situ in skin fibroblasts from patients with SSc.[53] Thus, our finding of PKD2 regulation of Akt has placed PKD2 in a central signaling network involved in dermal fibrosis. Interestingly, we noted that the basal levels of Akt and Stat3 were upregulated in the dermis, implying a potential compensatory mechanism for the loss of Akt activity. However, we did not detect any changes in Stat3 activity after BLM treatment in the KI mice, although IL-6 was downregulated. This finding suggests that PKD2 does not regulate the Stat3 signaling pathway in the context of dermal fibrosis.

Our study has also demonstrated the therapeutic benefit of a pan-PKD inhibitor in reversing BLM-induced fibrosis. The finding encourages further evaluation of PKD inhibitors as a potential treatment for dermal fibrosis. It also implies that other PKD isoforms may have redundant functions as PKD2; however, in light of their differential localization in the skin, the 3 isoforms may act through different mechanisms to promote the fibrotic process in the skin. Future studies on specific PKD isoforms will provide more insights into their roles and signaling mechanisms in dermal fibrosis and their involvement in the pathogenesis of SSc.

In summary, our results underline the importance of PKD2 catalytic activity in BLM-induced dermal fibrosis, suggesting that PKD2-positive myeloid cells may contribute to the production of profibrotic cytokines that promote dermal fibrosis induced by BLM. Given our promising data in the mouse model, PKD inhibitors may hold promise for treating skin inflammation and fibrosis in SSc.

Supplementary Material

Refer to Web version on PubMed Central for supplementary material.

Acknowledgments

The authors are truly thankful for Xuejing Zhang at the Department of Pharmacology and Chemical Biology, University of Pittsburgh, for her technical assistance in the completion of a real-time PCR experiment.

Funding

This study was supported in part by the American Heart Association (19TPA34850096 to Q.J.W.).

Data Availability

All data generated or analyzed during this study are included in this published article (and its supplementary information files).

References

1. Wei J, Zhu H, Lord G, et al. Nrf2 exerts cell-autonomous antifibrotic effects: compromised function in systemic sclerosis and therapeutic rescue with a novel heterocyclic chalcone derivative. Transl Res. 2017;183:71–86.e1. [PubMed: 28027929]
2. Gorkiewicz-Petkow A, Kalinska-Bienias A. Systemic involvement in localized scleroderma/morphea. Clin Dermatol. 2015;33(5):556–562. [PubMed: 26321403]
3. Smith GP, Chan ES. Molecular pathogenesis of skin fibrosis: insight from animal models. Curr Rheumatol Rep. 2010;12(1):26–33. [PubMed: 20425530]

4. Yamamoto T The bleomycin-induced scleroderma model: what have we learned for scleroderma pathogenesis? Arch Dermatol Res. 2006;297(8):333–344. [PubMed: 16402183]
5. Yamamoto T, Takagawa S, Katayama I, et al. Animal model of sclerotic skin. I: Local injections of bleomycin induce sclerotic skin mimicking scleroderma. J Invest Dermatol. 1999;112(4):456–462. [PubMed: 10201529]
6. Van Lint JV, Sinnett-Smith J, Rozengurt E. Expression and characterization of PKD, a phorbol ester and diacylglycerol-stimulated serine protein kinase. J Biol Chem. 1995;270(3):1455–1461. [PubMed: 7836415]
7. Zhang X, Connelly JA, Chao Y, et al. Multifaceted functions of protein kinase D in pathological processes and human diseases. Biomolecules. 2021;11(3):483. [PubMed: 33807058]
8. Yuan J, Pandol SJ. PKD signaling and pancreatitis. J Gastroenterol. 2016;51(7):651–659. [PubMed: 26879861]
9. Lavalle CR, Zhang L, Xu S, Eiseman JL, Wang QJ. Inducible silencing of protein kinase D3 inhibits secretion of tumor-promoting factors in prostate cancer. Mol Cancer Ther. 2012;11(7):1389–1399. [PubMed: 22532599]
10. Kim YI, Park JE, Brand DD, Fitzpatrick EA, Yi AK. Protein kinase D1 is essential for the proinflammatory response induced by hypersensitivity pneumonitis-causing thermophilic actinomycetes *Saccharopolyspora rectivirgula*. J Immunol. 2010;184(6):3145–3156. [PubMed: 20142359]
11. Yamashita K, Gon Y, Shimokawa T, et al. High affinity receptor for IgE stimulation activates protein kinase D augmenting activator protein-1 activity for cytokine producing in mast cells. Int Immunopharmacol. 2010;10(3):277–283. [PubMed: 19932769]
12. Salamon P, Shefler I, Hershko AY, Mekori YA. The involvement of protein kinase D in T cell-induced mast cell activation. Int Arch Allergy Immunol. 2016;171(3–4):203–208. [PubMed: 28049203]
13. Hao Q, Wang L, Tang H. Vascular endothelial growth factor induces protein kinase D-dependent production of proinflammatory cytokines in endothelial cells. Am J Physiol Cell Physiol. 2009;296(4):C821–C827. [PubMed: 19176759]
14. Yuan J, Liu Y, Tan T, et al. Protein kinase D regulates cell death pathways in experimental pancreatitis. Front Physiol. 2012;3:60. [PubMed: 22470346]
15. Thrower EC, Yuan J, Usmani A, et al. A novel protein kinase D inhibitor attenuates early events of experimental pancreatitis in isolated rat acini. Am J Physiol Gastrointest Liver Physiol. 2011;300(1):G120–G129. [PubMed: 20947701]
16. Xu X, Gera N, Li H, et al. GPCR-mediated PLCβγ/PKCβ/PKD signaling pathway regulates the cofilin phosphatase slingshot 2 in neutrophil chemotaxis. Mol Biol Cell. 2015;26(5):874–886. [PubMed: 25568344]
17. Xu X, Jin T. The novel functions of the PLC/PKC/PKD signaling axis in G protein-coupled receptor-mediated chemotaxis of neutrophils. J Immunol Res. 2015;2015, 817604. [PubMed: 26605346]
18. Murphy TR, Legere III HJ, Katz HR. Activation of protein kinase D1 in mast cells in response to innate, adaptive, and growth factor signals. J Immunol. 2007;179(11):7876–7882. [PubMed: 18025234]
19. Rezaee F, Desando SA, Ivanov AI, et al. Sustained protein kinase D activation mediates respiratory syncytial virus-induced airway barrier disruption. J Virol. 2013;87(20):11088–11095. [PubMed: 23926335]
20. Zheng H, Qian J, Varghese B, Baker DP, Fuchs S. Ligand-stimulated downregulation of the alpha interferon receptor: role of protein kinase D2. Mol Cell Biol. 2011;31(4):710–720. [PubMed: 21173164]
21. Fielitz J, Kim MS, Shelton JM, et al. Requirement of protein kinase D1 for pathological cardiac remodeling. Proc Natl Acad Sci U S A. 2008;105(8):3059–3063. [PubMed: 18287012]
22. Gan H, McKenzie R, Hao Q, Idell S, Tang H. Protein kinase D is increased and activated in lung epithelial cells and macrophages in idiopathic pulmonary fibrosis. PLoS One. 2014;9(7), e101983. [PubMed: 25000413]

23. Matthews SA, Navarro MN, Sinclair LV, Emslie E, Feijoo-Carnero C, Cantrell DA. Unique functions for protein kinase D1 and protein kinase D2 in mammalian cells. Biochem J. 2010;432(1):153–163. [PubMed: 20819079]
24. Xiong J, Zhou MF, Wang YD, et al. Protein kinase D2 protects against acute colitis induced by dextran sulfate sodium in mice. Sci Rep. 2016;6, 34079. [PubMed: 27659202]
25. Kitaba S, Murota H, Terao M, et al. Blockade of interleukin-6 receptor alleviates disease in mouse model of scleroderma. Am J Pathol. 2012;180(1):165–176. [PubMed: 22062222]
26. Xu W, Zeng F, Li S, et al. Crosstalk of protein kinase C epsilon with Smad2/3 promotes tumor cell proliferation in prostate cancer cells by enhancing aerobic glycolysis. Cell Mol Life Sci. 2018;75(24):4583–4598. [PubMed: 30209539]
27. Faul F, Erdfelder E, Lang A, et al. G*Power 3: a flexible statistical power analysis program for the social, behavioral, and biomedical sciences. Behav Res Methods. 2007;39(2):175–191. [PubMed: 17695343]
28. Sturany S, Van Lint J, Gilchrist A, Vandenheede JR, Adler G, Seufferlein T. Mechanism of activation of protein kinase D2(PKD2) by the CCK(B)/gastrin receptor. J Biol Chem. 2002;277(33):29431–29436. [PubMed: 12058027]
29. Bhattacharyya S, Tamaki Z, Wang W, et al. Fibronectin^{EDA} promotes chronic cutaneous fibrosis through toll-like receptor signaling. Sci Transl Med. 2014;6(232):232ra50.
30. Cazalets C, Cador B, Rolland Y, et al. [Digital flow exploration by color Doppler ultrasound in patients with Raynaud's disease or systemic sclerosis]. J Mal Vasc. 2004;29(1):12–20. [PubMed: 15094661]
31. Zvaifler NJ. Relevance of the stroma and epithelial-mesenchymal transition (EMT) for the rheumatic diseases. Arthritis Res Ther. 2006;8(3):210. [PubMed: 16689999]
32. Zurita-Salinas CS, Krotzsch E, Diaz de Leon L, Alcocer-Varela J. Collagen turnover is diminished by different clones of skin fibroblasts from early- but not late-stage systemic sclerosis. Rheumatol Int. 2004;24(5):283–290. [PubMed: 14600784]
33. Jelaska A, Korn JH. Role of apoptosis and transforming growth factor β1 in fibroblast selection and activation in systemic sclerosis. Arthritis Rheum. 2000;43(10):2230–2239. [PubMed: 11037882]
34. Borges S, Perez EA, Thompson EA, Radisky DC, Geiger XJ, Storz P. Effective targeting of estrogen receptor-negative breast cancers with the protein kinase D inhibitor CRT0066101. Mol Cancer Ther. 2015;14(6):1306–1316. [PubMed: 25852060]
35. Harikumar KB, Kunnumakkara AB, Ochi N, et al. A novel small-molecule inhibitor of protein kinase D blocks pancreatic cancer growth in vitro and in vivo. Mol Cancer Ther. 2010;9(5):1136–1146. [PubMed: 20442301]
36. Wei N, Chu E, Wipf P, Schmitz JC. Protein kinase D as a potential chemotherapeutic target for colorectal cancer. Mol Cancer Ther. 2014;13(5):1130–1141. [PubMed: 24634417]
37. Bergmann C, Brandt A, Merlevede B, et al. The histone demethylase Jumonji domain-containing protein 3 (JMJD3) regulates fibroblast activation in systemic sclerosis. Ann Rheum Dis. 2018;77(1):150–158. [PubMed: 29070530]
38. Furue M, Mitoma C, Mitoma H, et al. Pathogenesis of systemic sclerosis-current concept and emerging treatments. Immunol Res. 2017;65(4):790–797. [PubMed: 28488090]
39. Distler O, Cozzio A. Systemic sclerosis and localized scleroderma—current concepts and novel targets for therapy. Semin Immunopathol. 2016;38(1):87–95. [PubMed: 26577237]
40. Zhang S, Liu H, Yin M, et al. Deletion of protein kinase D3 promotes liver fibrosis in mice. Hepatology. 2020;72(5):1717–1734. [PubMed: 32048304]
41. Tamby MC, Chanseaud Y, Guillevin L, Mouthon L. New insights into the pathogenesis of systemic sclerosis. Autoimmun Rev. 2003;2(3):152–157. [PubMed: 12848956]
42. Abraham DJ, Varga J. Scleroderma: from cell and molecular mechanisms to disease models. Trends Immunol. 2005;26(11):587–595. [PubMed: 16168711]
43. Baraut J, Farge D, Jean-Louis F, et al. Transforming growth factor-β increases interleukin-13 synthesis via GATA-3 transcription factor in T-lymphocytes from patients with systemic sclerosis. Arthritis Res Ther. 2015;17:196. [PubMed: 26227022]

44. Ningyan G, Xu Y, Hongfei S, Jingjing C, Min C. The role of macrophage migration inhibitory factor in mast cell-stimulated fibroblast proliferation and collagen production. PLOS ONE. 2015;10(3), e0122482. [PubMed: 25826375]
45. Terao M, Yang L, Matsumura S, Yutani M, Murota H, Katayama I. A vitamin D analog inhibits Th2 cytokine- and TGFβ-induced periostin production in fibroblasts: a potential role for vitamin D in skin sclerosis. Dermatoendocrinol. 2015;7(1), e1010983. [PubMed: 26413189]
46. Vorstenbosch J, Nguyen CM, Zhou S, et al. Overexpression of CD109 in the epidermis differentially regulates ALK1 versus ALK5 signaling and modulates extracellular matrix synthesis in the skin. J Invest Dermatol. 2017;137(3):641–649. [PubMed: 27866969]
47. Liu Q, Chu H, Ma Y, et al. Salvianolic acid B attenuates experimental pulmonary fibrosis through inhibition of the TGF-β signaling pathway. Sci Rep. 2016;6, 27610. [PubMed: 27278104]
48. Muangchant C, Pope JE. The significance of interleukin-6 and C-reactive protein in systemic sclerosis: a systematic literature review. Clin Exp Rheumatol. 2013;31(2 suppl 76):122–134.
49. Wang J, Hu K, Cai X, et al. Targeting PI3K/AKT signaling for treatment of idiopathic pulmonary fibrosis. Acta Pharm Sin B. 2022;12(1):18–32. [PubMed: 35127370]
50. Teng Y, Fan Y, Ma J, et al. The PI3K/Akt pathway: emerging roles in skin homeostasis and a group of non-malignant skin disorders. Cells. 2021;10(5).
51. Bignold R, Johnson JR. Effects of cytokine signaling inhibition on inflammation-driven tissue remodeling. Curr Res Pharmacol Drug Discov. 2021;2, 100023. [PubMed: 34909658]
52. Lofgren S, Hinchcliff M, Carns M, et al. Integrated, multicohort analysis of systemic sclerosis identifies robust transcriptional signature of disease severity. JCI Insight. 2016;1(21), e89073. [PubMed: 28018971]
53. Jun JB, Kuechle M, Min J, et al. Scleroderma fibroblasts demonstrate enhanced activation of Akt (protein kinase B) in situ. J Invest Dermatol. 2005;124(2):298–303. [PubMed: 15675946]
54. Schneider CA, Rasband WS, Eliceiri KW. NIH Image to ImageJ: 25 years of image analysis. Nat Methods. 2012;9:671–675. [PubMed: 22930834]

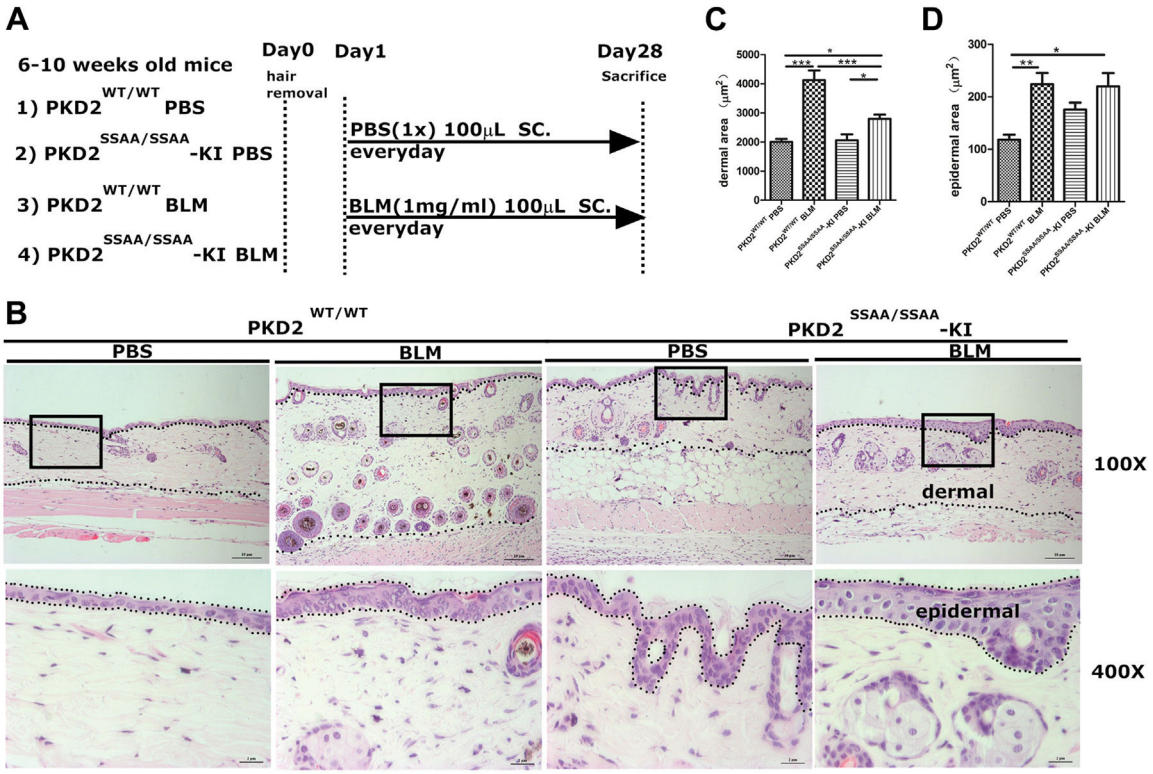

Figure 1.

PKD2$^{SSAA/SSAA}$-KI mice were resistant to BLM-induced dermal fibrosis. (A) Diagram depicting a mouse model of BLM-induced fibrosis. Briefly, 4 groups of mice were subjected to daily s.c. injection of 100 μL of PBS or BLM (1 mg/mL) for 28 days (n = 9). (B) Representative images of H&E-stained skin sections from PKD2$^{WT/WT}$ mice or PKD2$^{SSAA/SSAA}$-KI mice injected with PBS or BLM. Regions between the dotted lines are the measured areas of the dermal layer or the epidermal layer. The black box indicates the position of ×400 images. Original magnifications: ×100, scale display 10 μm; ×400, scale display 2 μm. (C, D) The dermal and epidermal thicknesses were measured using ImageJ[54] software. Data are shown as the means ± SD of triplicate determinations per ×100 image from 9 mice per group. Statistical significance was analyzed using one-way analysis of variance with multiple comparisons. *P < .05, ***P < .001. BLM, bleomycin; H&E, hematoxylin and eosin; KI, knock-in; PBS, phosphate-buffered saline; PKD2, protein kinase D2; s.c., subcutaneous.

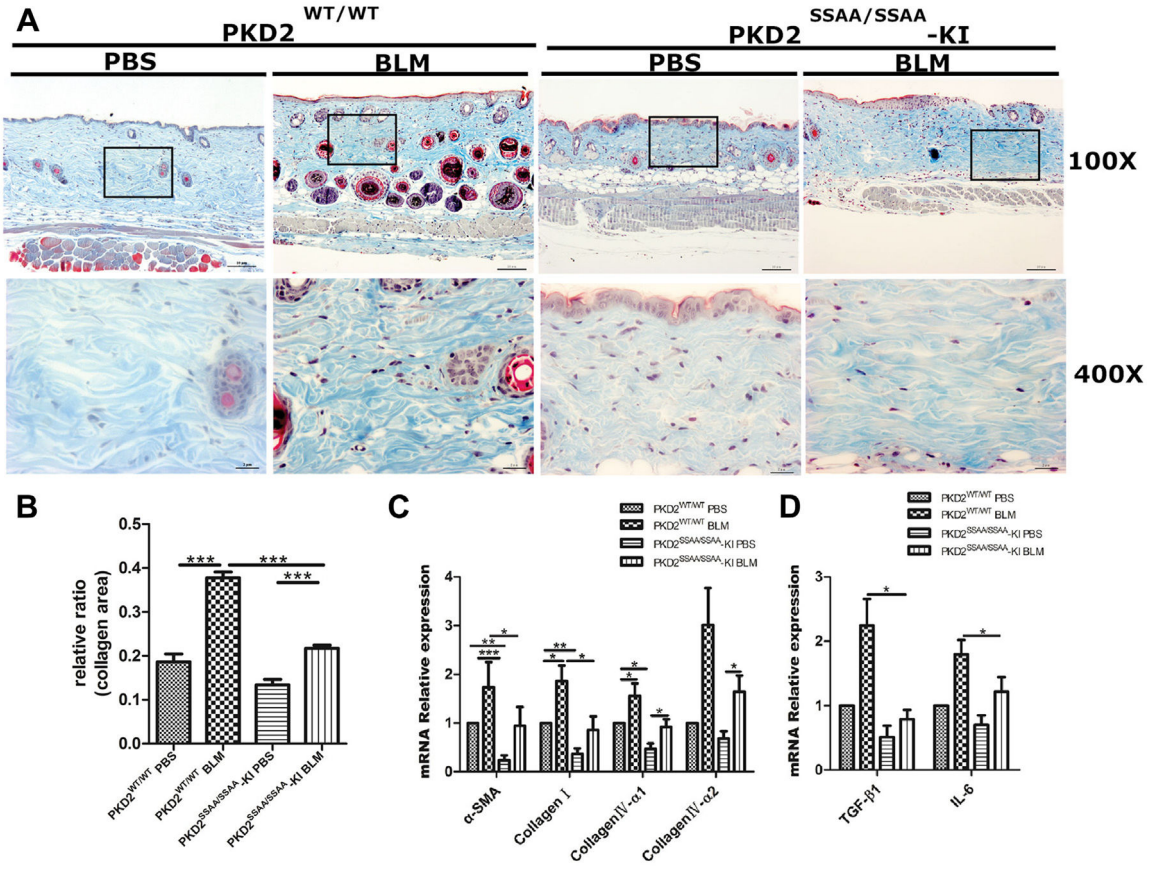

Figure 2.

PKD2$^{SSAA/SSAA}$-KI mice showed reduced collagen fibers as well as α-SMA, collagen, TGF-β1, and IL-6 gene expression in the dermis after BLM treatment. (A) Masson trichrome staining of skin sections from PKD2$^{WT/WT}$ or PKD2$^{SSAA/SSAA}$-KI mice injected with PBS or BLM. Collagen fibers were stained blue and the nuclei were stained black. The black boxes indicate the position of ×400 images. Original magnifications: ×100, scale display 10 μm; ×400, scale display 2 μm. (B) The relative ratio (%) of collagen fibers of 4 groups measured using Image J software and analyzed using one-way analysis of variance with multiple comparisons. $^{**}P < .01$, $^{***}P < .001$. (C, D) mRNA expression of α-SMA, collagen, TGF-β1, and IL-6. The total RNA of skin samples from indicated groups was extracted and mRNA levels of α-SMA, collagen I, collagen IV-α1, collagen IV-α2, TGF-β1, and IL-6 were measured using real-time RT-qPCR with GAPDH as the internal control. Data represent the means ± SD of 9 mice per group and were analyzed using one-way analysis of variance with multiple comparisons. $^{*}P < .05$, $^{**}P < .01$, $^{***}P < .001$. BLM, bleomycin; GAPDH, glyceraldehyde-3-phosphate dehydrogenase; IL-6, interleukin-6; KI, knock-in; PBS, phosphate-buffered saline; PKD2, protein kinase D2; RT-qPCR, real-time reverse-transcription PCR; α-SMA, α-smooth muscle actin; TGF-β1, transforming growth factor-β1.

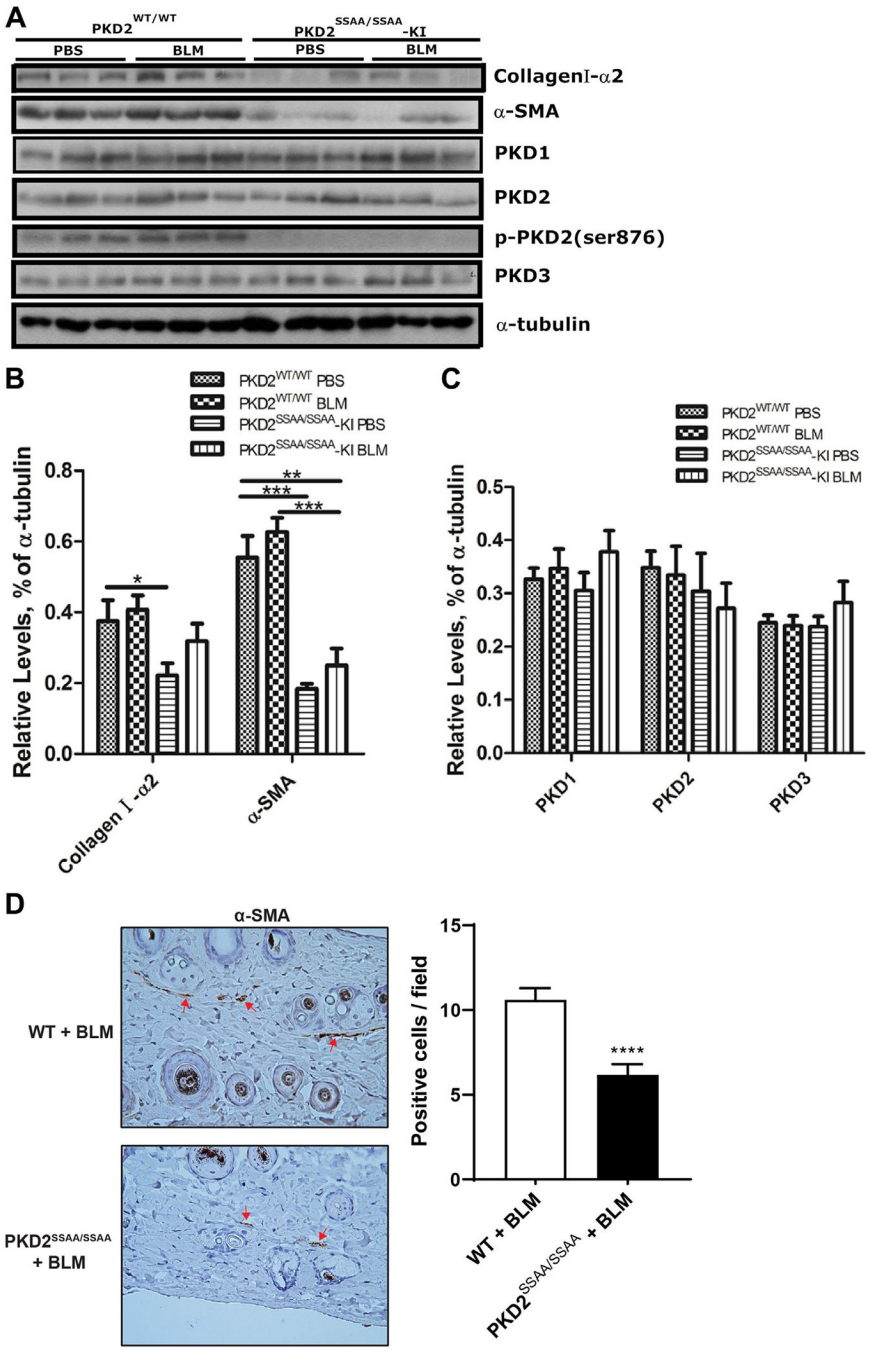

Figure 3.

PKD2$^{SSAA/SSAA}$-KI mice exhibited reduced collagen I-α2 and α-SMA protein expression and the absence of PKD2 activities. (A) Western blot analysis of the skin samples. KI and WT mice (n = 9) were subjected to daily s.c. injection of 100 μL of PBS or BLM (1 mg/mL) for 28 days. Skin samples were lysed and analyzed by Western blotting for the expression of α-SMA, collagen I-α2, p-PKD2 (S876), and native PKD isoforms. α-Tubulin was blotted as the loading control. (B, C) Corresponding densitometric quantifications of collagen I-α2, α-SMA, PKD1, PKD2, and PKD3 levels in Western blots using ImageJ software and

analyzed using one-way analysis of variance with multiple comparisons. Data represent the means ± SD from 9 mice per group. *$P < .05$, **$P < .01$, ***$P < .001$. (D) Reduced number of α-SMA–positive cells in the mouse skin of BLM-treated KI mice compared with that in WT mice. Mouse skin sections were analyzed by IHC using α-SMA antibody. Right, representative IHC images, ×400; left, quantitative analysis of α-SMA–positive cells in the dermis from 6 to 10 random fields. Mean ± SD values are shown. ****$P < .0001$. BLM, bleomycin; IHC, immunohistochemistry; KI, knock-in; PBS, phosphate-buffered saline; PKD, protein kinase D; s.c., subcutaneous; α-SMA, α-smooth muscle actin; WT, wild-type.

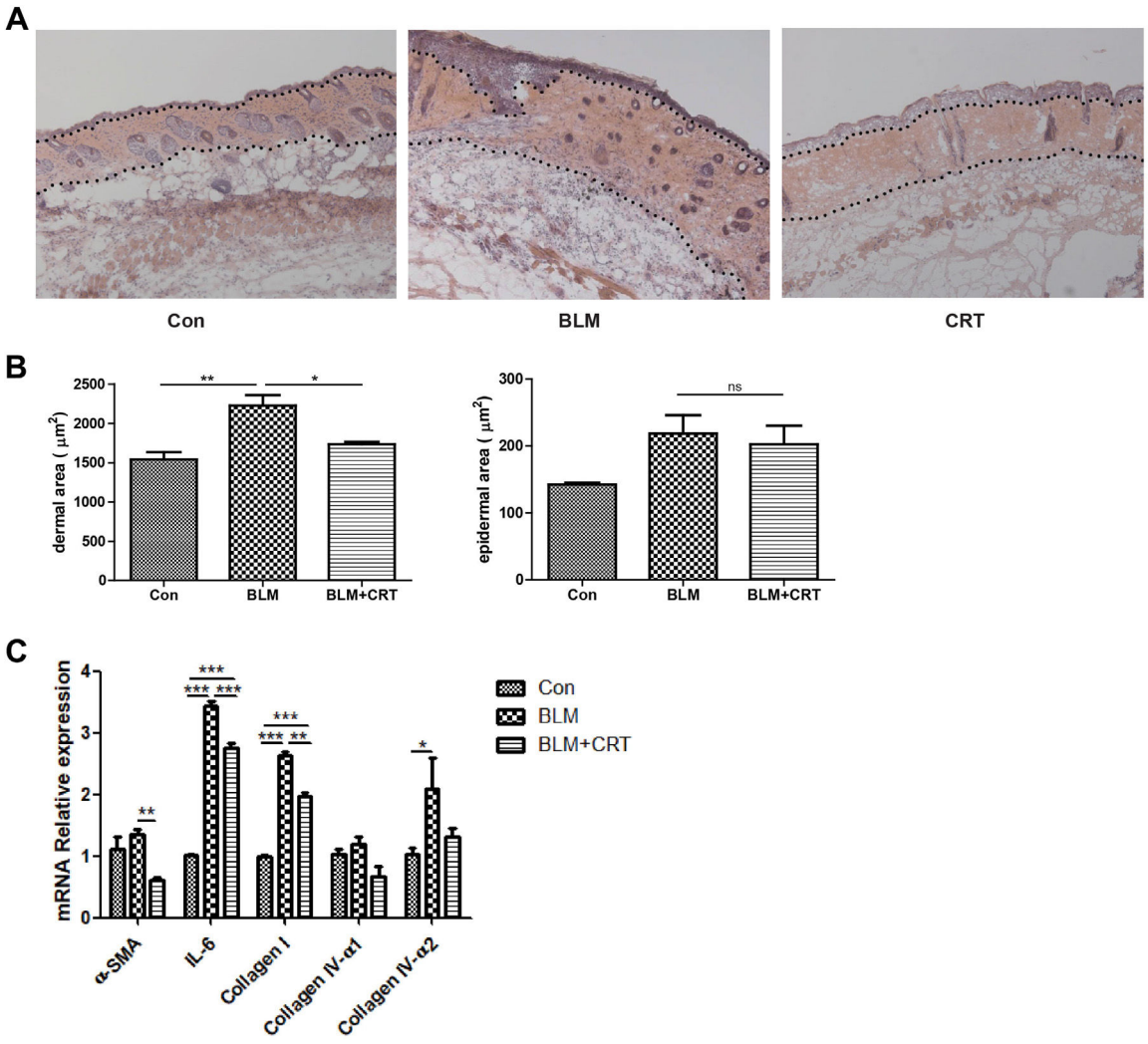

Figure 4.

Inhibition of PKD blocked BLM-induced dermal fibrosis in mice. Healthy mice were randomized into 3 groups (n = 6) and subjected to daily s.c. injections of PBS, BLM (1 mg/mL), and BLM + CRT (80 mg/kg) for 28 days. At the end of the treatment, the skin around the injection site was harvested, sectioned, and subjected to H&E staining. (A) Representative images of H&E-stained skin sections from mice. Regions between the dotted lines are the measured areas of the dermal layer. Original magnification: ×100. (B) The dermal and epidermal thicknesses were measured using ImageJ software. Data are shown as the means ± SD of triplicate determinations per image from 6 mice per group. Statistical significance was analyzed using one-way analysis of variance with multiple comparisons. $*P < .05$, $***P < .001$. (C) Total RNA of skin samples from indicated groups was extracted and mRNA levels of α-SMA, collagen I, collagen IV-α1, collagen IV-α2, and IL-6 were measured using real-time RT-qPCR with GAPDH as the internal control. Data represent the means ± SD of 6 mice per group and were analyzed using one-way analysis of variance with multiple comparisons. $*P < .05$, $**P < .01$, $***P < .001$. BLM, bleomycin; CRT, CRT0066101; GAPDH, glyceraldehyde-3-phosphate dehydrogenase; H&E, hematoxylin

and eosin; IL-6, interleukin-6; ns, not significant; PBS, phosphate-buffered saline; PKD, protein kinase D; RT-qPCR, real-time reverse-transcription PCR; s.c., subcutaneous; α-SMA, α-smooth muscle actin.

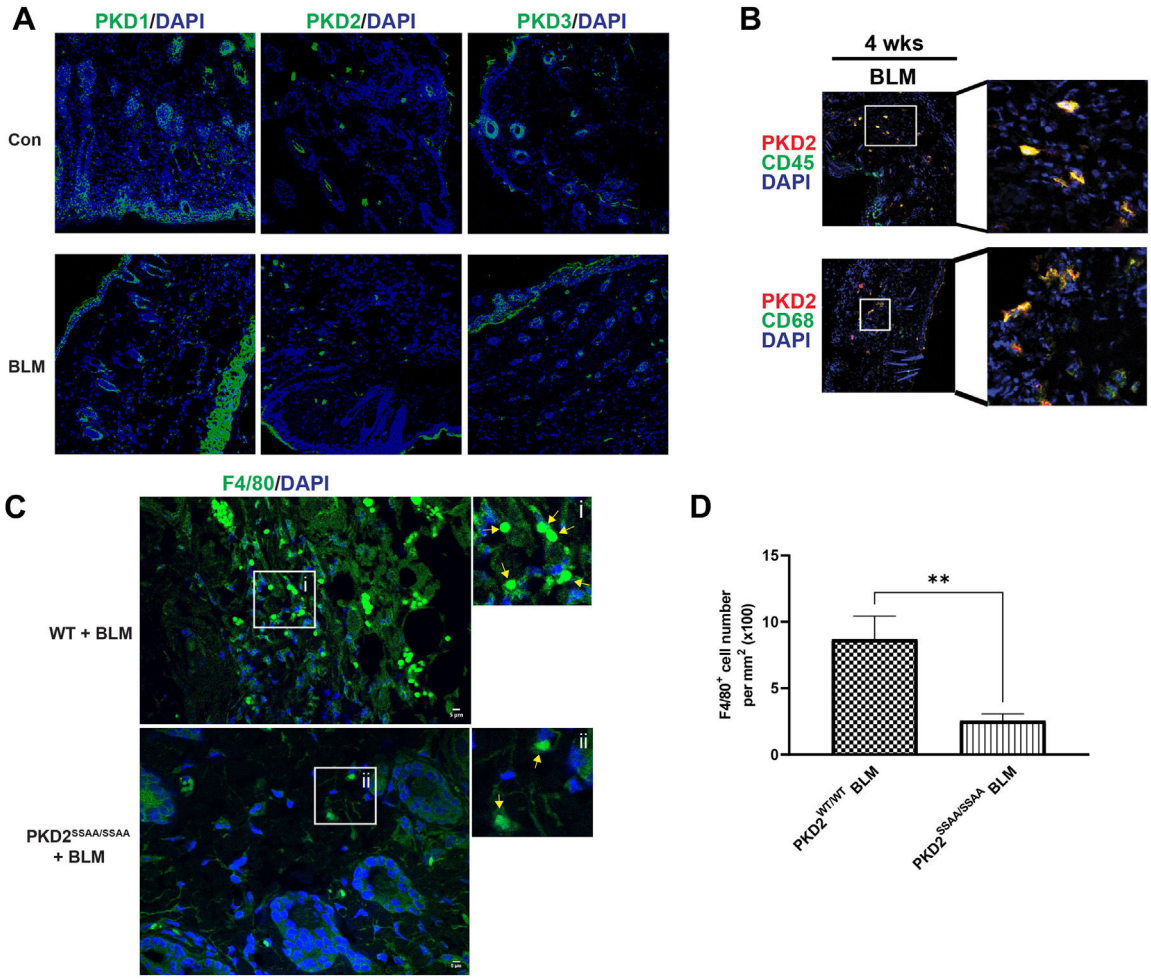

Figure 5.

PKD2 resided in macrophages recruited to the lesional skin. (A) PKD1/2/3 distribution in mouse skin before and after BLM treatment. Frozen skin sections from mice treated with PBS (con) or BLM for 4 weeks were subjected to IF staining using PKD1/2/3 antibodies. Representative merged images are shown. Green, PKD1/2/3; blue, DAPI. Original magnification: ×100. (B) PKD2 resided in $CD45^{+}/CD68^{+}$ myeloid cells in the dermis of BLM-treated mice. Frozen tissue sections from 4-week BLM-treated mice were costained with PKD2 (red) and CD45 (green) or CD68 (green) and counterstained with DAPI (blue). Original magnification: ×100. (C) The loss of PKD2 activity reduced the recruitment of F4/80+ macrophages in the dermis of BLM-treated mice. KI and WT mice (n = 3) were subjected to a daily s.c. injection of 100 μL of BLM (1 mg/mL) for 1 week. Skin sections from BLM-treated WT and KI mice were analyzed by IF staining using the anti-F4/80 antibody and counterstained with DAPI. Original magnification: ×630. Representative images are shown. Regions i-ii are enlarged (right). Yellow arrows indicate F4/80+ cells. (D) The quantitative measure of F4/80+ macrophages in KI and WT mouse skin sections. F4/80+ cells in 5 to 7 random fields were counted for each tissue section. Mean ± SD values are shown. $^{**}P < .01$. BLM, bleomycin; IF, immunofluorescence; KI, knock-in; PBS, phosphate-buffered saline; PKD, protein kinase D; WT, wild-type.

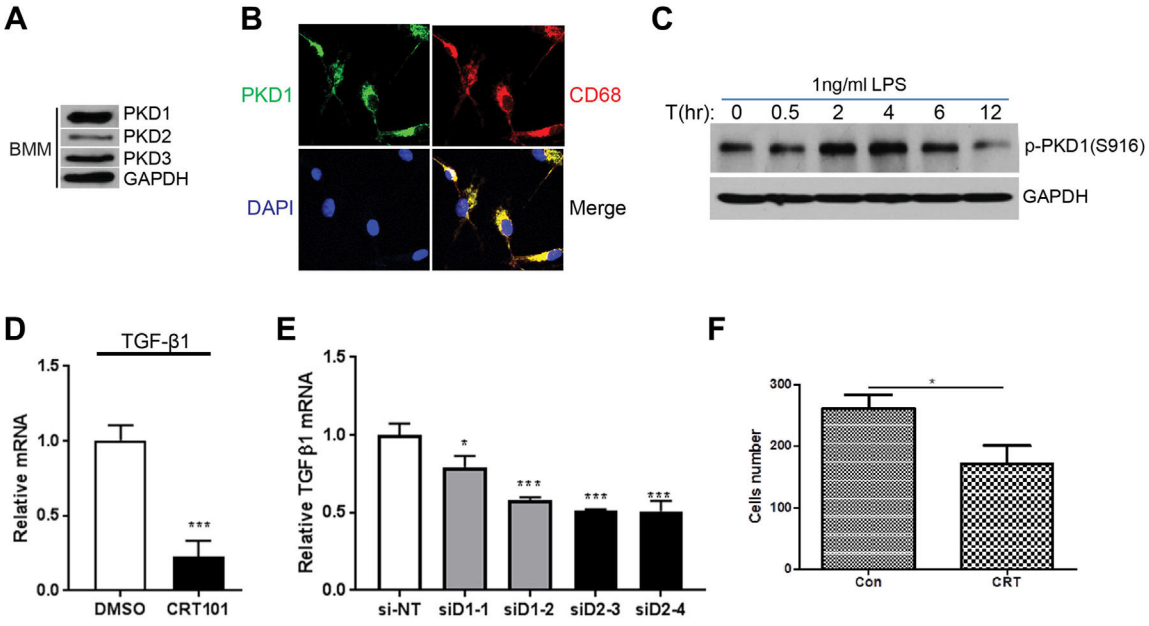

Figure 6.

PKD was required for BMM migration and LPS-stimulated cytokine production. (A) Expression of PKD isoforms in BMMs. Cell lysates of BMMs were analyzed by immunoblotting for PKD isoforms. (B) BMMs were positive for CD68. BMMs were costained with PKD1 (green) and CD68 (red), and counterstained with DAPI (blue). Representative images are shown. Original magnification: x100. (C) LPS activated PKD1. BMMs were stimulated with 1 ng/mL of LPS for different times. Cells were lysed and subjected to immunoblotting for p-PKD1(S916). (D) Effects of CRT on LPS-induced TGF-β1 expression in BMMs. BMMs were stimulated with 1 ng/mL of LPS for 4 hours. CRT (2 μM) was added in the last 2 hours of LPS treatment. Cells were analyzed for TGF-β1 mRNA using real-time RT-qPCR. (E) Knockdown of PKD1 or PKD2 decreased LPS-induced TGF-β1 expression in BMMs. BMMs were transfected with PKD1 (siD1–1 and -2) and PKD2 (siD2–1 and -2) siRNAs. Two days after transfection, the cells were stimulated with 1 ng/mL of LPS for 4 hours and subjected to real-time RT-qPCR analysis for TGF-b1 mRNA expression. (F) CRT-blocked BMM migration. BMM, bone marrow–derived macrophage; CRT, CRT0066101; LPS, lipopolysaccharide; PKD, protein kinase D; RT-qPCR, real-time reverse-transcription PCR; siRNA, small interfering RNA; TGF-β1, transforming growth factor-β1.

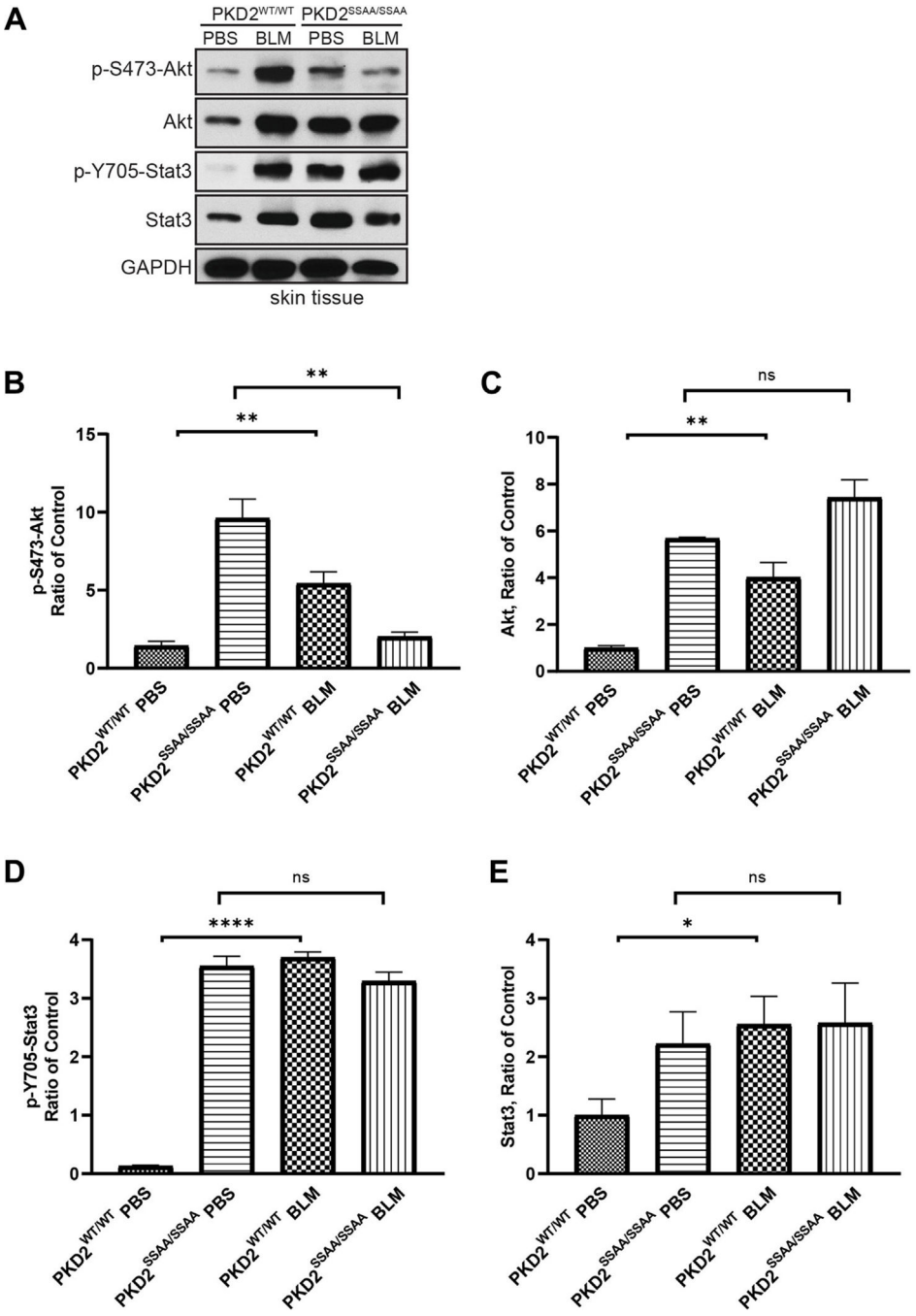

Figure 7.

PKD2 activity was required for BLM-induced Akt activation in the early inflammatory phase. (A) Western blot analysis of mouse skin samples. KI and WT mice (n = 3) were subjected to a daily s.c. injection of 100 μL of BLM (1 mg/mL) for 7 days. Skin samples were lysed and immunoblotted for the indicated proteins. GAPDH was blotted as the loading control. (B-E) Corresponding densitometric quantifications of p-S473-Akt, Akt, p-Y705-Stat3, and Stat3 levels using ImageJ software. Data represent the mean ± SD from 3 separate experiments. *$P < .05$, **$P < .01$, ****$P < .0001$. BLM, bleomycin; GAPDH,

glyceraldehyde-3-phosphate dehydrogenase; KI, knock-in; ns, not significant; PKD, protein kinase D; s.c., subcutaneous; WT, wild-type.

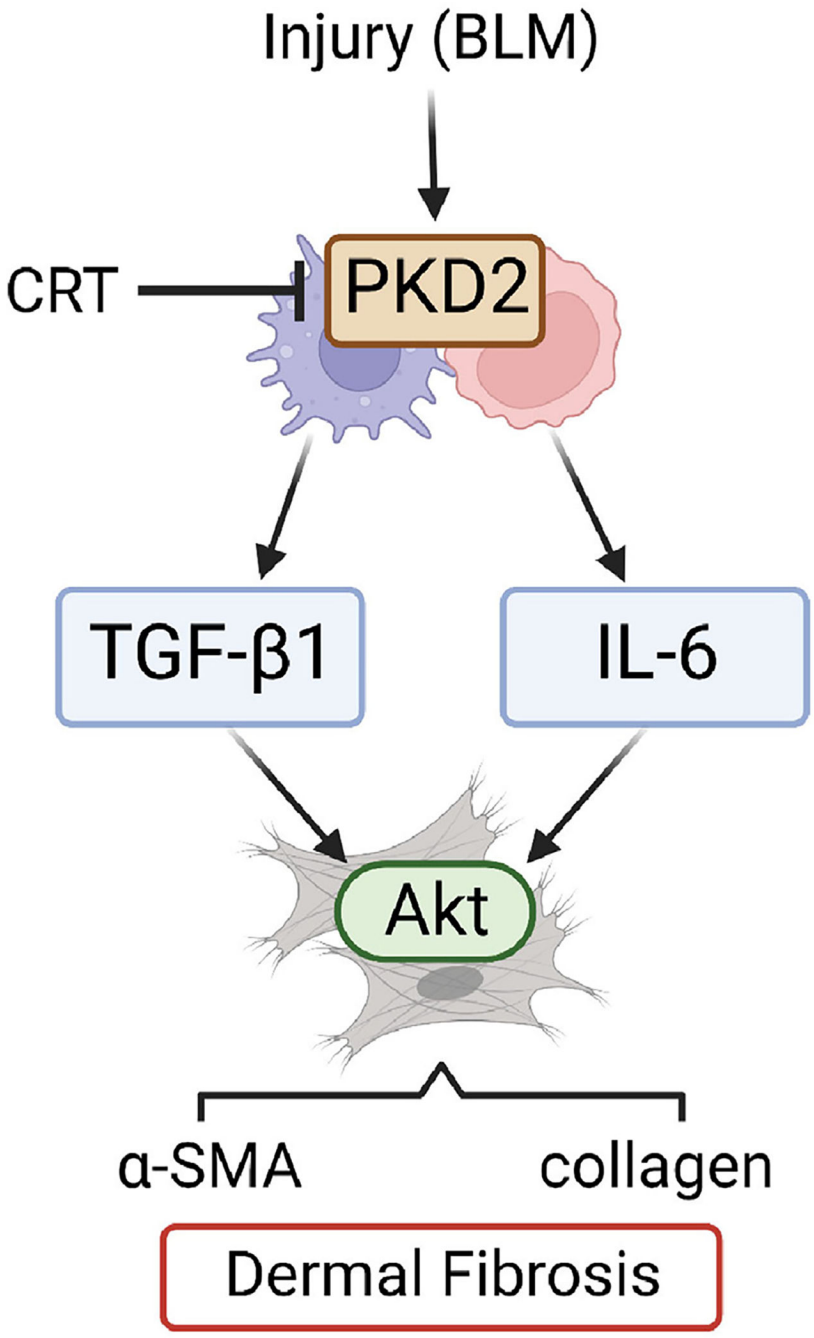

Figure 8.

A diagram depicting the potential signaling mechanisms of PKD2 in dermal fibrosis. A BLM-induced injury activates PKD2, which promotes the recruitment of monocytes/macrophages and the production of proinflammatory and profibrotic cytokines from these cells at the lesional sites, which further activates Akt, resulting in increased myofibroblastic activity, collagen deposition, and thickening of the skin. This pathologic process could be blocked by a PKD inhibitor CRT. α-SMA, α-smooth muscle actin; BLM, bleomycin; CRT,

CRT0066101; IL-6, interleukin-6; PKD, protein kinase D; TGF-β1, transforming growth factor-β1. The diagram is created with BioRender.com.